

## ESA Technical Note (December 2019):

### CCN#2: Support to MIPAS level 2 processor verification and validation – Phase F

#### Long-term validation of MIPAS ESA operational products using ACE v3/v4 measurements

David Moore and John Remedios

University of Leicester (UL)

#### Contents

1	Introduction .....	2
2	Instruments and data analysis .....	2
2.1	MIPAS instrument and data .....	2
2.2	ACE instrument and data .....	3
2.3	Validation methodology.....	4
3	Intercomparison results .....	5
3.1	Ozone (O <sub>3</sub> ) .....	6
3.2	Nitric Acid (HNO <sub>3</sub> ) .....	7
3.3	Carbonyl Fluoride (COF <sub>2</sub> ).....	8
3.4	Carbon Tetrachloride (CCl <sub>4</sub> ) .....	9
3.5	Hydrogen Cyanide (HCN) .....	10
3.6	Acetylene (C <sub>2</sub> H <sub>2</sub> ).....	11
3.7	Ethane (C <sub>2</sub> H <sub>6</sub> ).....	12
3.8	Chloromethane (CH <sub>3</sub> Cl).....	14
3.9	Phosgene (COCl <sub>2</sub> ) .....	15
3.10	Heavy Water (HDO).....	17
4	Conclusions .....	21
5	References .....	21

## 1 Introduction

The European Space Agency's (ESA's) Michelson Interferometer for Passive Atmospheric Sounding (MIPAS) operated for a decade between 2002 and 2012 measuring a number of key trace gases in the upper troposphere and stratosphere, linked to a changing climate and atmospheric chemistry. The validation of these data is an essential task to determine the accuracy and precision of these measurements over the lifetime of the mission. Validation is often performed against in-situ data from aircraft or ground-based data. In this work, data are compared to another satellite dataset; the Atmospheric Chemistry Experiment (ACE) onboard SCISAT-1. The main issue with validating between different satellite instruments flying in a different orbit, is careful selection of matchups to minimize the time and distance between the two satellite measurements. In the following sections, the satellite datasets are introduced, validation activities and validation results are described in detail.

## 2 Instruments and data analysis

### 2.1 MIPAS instrument and data

The MIPAS-E instrument was successfully launched onboard the ENVironmental SATellite (ENVISAT) in March 2002 as part of an ambitious and innovative payload. The ENVISAT measured from a polar orbit at an altitude of 800 km, with an orbital period of about 100 min and a reference orbit repeat cycle of 35 days. The MIPAS onboard Envisat (Fischer and Oelhaf, 1996; Fischer et al., 2008) is a Fourier Transform Spectrometer that was designed to provide continual limb emission measurements in the mid infrared over the range 685–2410  $\text{cm}^{-1}$  (14.6–4.15  $\mu\text{m}$ ) at an unapodized resolution of 0.025  $\text{cm}^{-1}$ . The instrument's field of view is approximately 3×30×400 km and one complete limb sequence of measurements in full-resolution nominal mode consisted of 17 spectra with tangent altitudes at 68 km, 60 km, 52 km, 47 km, 42 km and continuing downwards to 6 km in 3 km intervals. After commissioning the MIPAS was run predominantly in the full-resolution mode (FR mode) from July 2002 until March 2004. During this period the processing was performed by the ESA Instrument Processing Facilities (IPF) V4.1 and V4.2, based on the Optimized Retrieval Model (ORM) code described in Ridolfi et al. (2000) and in Raspollini et al. (2006), and covered the parameters p, T, and the six constituents H<sub>2</sub>O, O<sub>3</sub>, CH<sub>4</sub>, N<sub>2</sub>O, HNO<sub>3</sub>, and NO<sub>2</sub>. Previous validation studies of these species included: p, T (Ridolfi et al., 2007); O<sub>3</sub> (Cortesi et al., 2007); HNO<sub>3</sub> (Wang et al., 2007); NO<sub>2</sub> (Wetzel et al., 2007); N<sub>2</sub>O and CH<sub>4</sub> (Payan et al. 2009); H<sub>2</sub>O (Wetzel et al., 2013).

During late 2003, the interferometer drive of the MIPAS developed an increased frequency of problems and in March 2004 the data from instrument was suspended for more detailed investigations. By January 2005, the instrument was switched back to operation with a reduced maximum optical difference but the same interferogram scan speed which had the effect of reducing the spectral resolution by 41% of the nominal. A benefit of the new scan pattern was increased vertical scanning and more profiles per orbit of operation. Data from 2005 onwards are referred to as optimised resolution mode (OR mode), optimised in terms of a trade-off between spectral and spatial resolution and instrument operation safety. Data were run in OR mode until 8 April 2012 when an ENVISAT anomaly occurred and communication between the ground and the satellite was lost (ESA, 2012). Details of the characteristics of the two MIPAS mission phases (FR and OR modes) in terms of instrument settings and atmospheric sampling are described in Raspollini et al. (2013).

The changes during the OR mode meant a number of changes to the processing codes were needed, leading to the ESA Level 2 processor version 6 (Raspollini et al., 2013). This version also provided error estimates from the approach of Dudhia et al. (2002). Later versions of the processor included v7 and

v8. Data from the whole data period of ten years were processed using v6-v8. The high resolution of the MIPAS allowed the investigation of extra species to the nominal 6. Version 6 extended to ClONO<sub>2</sub>, N<sub>2</sub>O<sub>5</sub>, CFC-11 and CFC-12. The version 7, released in 2015, added HCN, HCFC-22, CF<sub>4</sub>, COF<sub>2</sub> and CCl<sub>4</sub>. An ESA L1v8/ L2v8 “diagnostic dataset” (DDS) was released in June 2018 followed by a full mission reprocessing in June 2019. The v8 data added in the molecules C<sub>2</sub>H<sub>2</sub>, C<sub>2</sub>H<sub>6</sub>, OCS, CH<sub>3</sub>Cl, and HDO. Validation of the full mission v8 data processing only are considered in this validation report.

For validation of the operational HDO product, this study compares to a research data product developed at the Karlsruhe Institut für Technologie (KIT), based largely on the work outlined in Lossow et al. 2011, with further updates since then, but still retrieved using the IMK/IAA processor. The retrieval employs a non-linear least square approach, with Tikhonov-type regulation to avoid unphysical oscillations in the profile. Radiative transfer through the atmosphere is modelled by the KOPRA (Karlsruhe Optimized and Precise Radiative Transfer Algorithm) model (Stiller et al., 2000).

## 2.2 ACE instrument and data

The Atmospheric Chemistry Experiment (ACE) on SCISAT was launched in August 2003 into an orbit at 650 km and 74-degree inclination angle to the equator, which produces a high density of measurements over high latitude regions (Bernath, 2017). The satellite is still operational in late 2019. The instrument onboard SCISAT relevant for the MIPAS validation work is the infrared solar-occultation Fourier Transform Spectrometer, measuring 750 to 4400 cm<sup>-1</sup> at a spectral resolution of 0.02 cm<sup>-1</sup>. The ACE-FTS can make up to 15 sunrise and 15 sunset observations per day. The vertical resolution of about 4 km extends from the mid-troposphere (5 km) up to 150 km. There are small data gaps (two weeks at a time) where the satellite’s orbit geometry prevent a full view of the sun.

Two versions of the ACE full-mission processing datasets are relevant to this validation; version 3.5/6 and v4.0. The largest differences between the two datasets is the use of updated spectroscopy in v4.0 and some changes to trace gas microwindow selection. Version 3.5 (February 2004 to March 2013) and version 3.6 (November 2012 onwards) are similar, and differences will be described here. Version 3.5/6 improved pressure and temperature from the Canadian Meteorological Center’s global model and the recommendation was to not use any products before v3.5. Only changes relevant to the MIPAS/ACE validation work between the two data versions are outlined here.

Generating the Level 1 data for version 4.0 filtered the high sun and deep space measurements for excessive noise, averaged over +/- 3 orbits (unlike v3.5) which should have had the effect of reducing the variability and/or oscillations in the retrieved profiles. This also had the benefit of recovering occultations that had no reference spectra, reducing noise and increasing the number of occultations. The failure rates using updated spectroscopy in v4.0 should be reduced. A new source of solar and geomagnetic data was implemented in v4.0 with the later years of v3.6 data only using nominal values for these quantities because the previous sources used were discontinued. These quantities are used in calculation of high altitude pressure and temperature profiles, which should improve retrieval results at high altitudes. Tangent altitude in v4.0 are determined from the N<sub>2</sub> continuum, meaning that altitude CO<sub>2</sub> can be retrieved. V3.5 and v4.0 contain all gases relevant to this validation. Results from ACE are not constrained to be positive and for VMRs close to zero, it is common to retrieve negative values. Averaged results should come out to be positive, or zero if there is no signal.

### 2.3 Validation methodology

ACE has been operational since 2004 and therefore only measurements in the MIPAS “optimised resolution” phase are considered in this analysis from January 2005 onwards. Only MIPAS data in the 27 level nominal mode are considered and ACE data which are not considered a priori values are included. Due to the retrieval approach of ACE, negative values can occur in the retrieval process, whilst not being physically possible are mathematically possible. Negative values are left in the analysis. As the ACE provides only up to 30 measurements per day, in specific regions, this presented some challenges for validation, for example matchups in the tropics (20S-20N) are only obtained with very loose matchup criteria in both space and time, which leads to misinterpretation of results for short-lived species. Therefore we restrict analysis to “global” comparisons understanding that the scan pattern of the ACE instrument is such that most of the Northern Hemisphere measurements are over latitudes of Canada (due to Canadian Space Agency funding). The scan pattern of ACE for 2015 is shown in Figure 1, and is very similar year-to-year (Bernath, 2017).

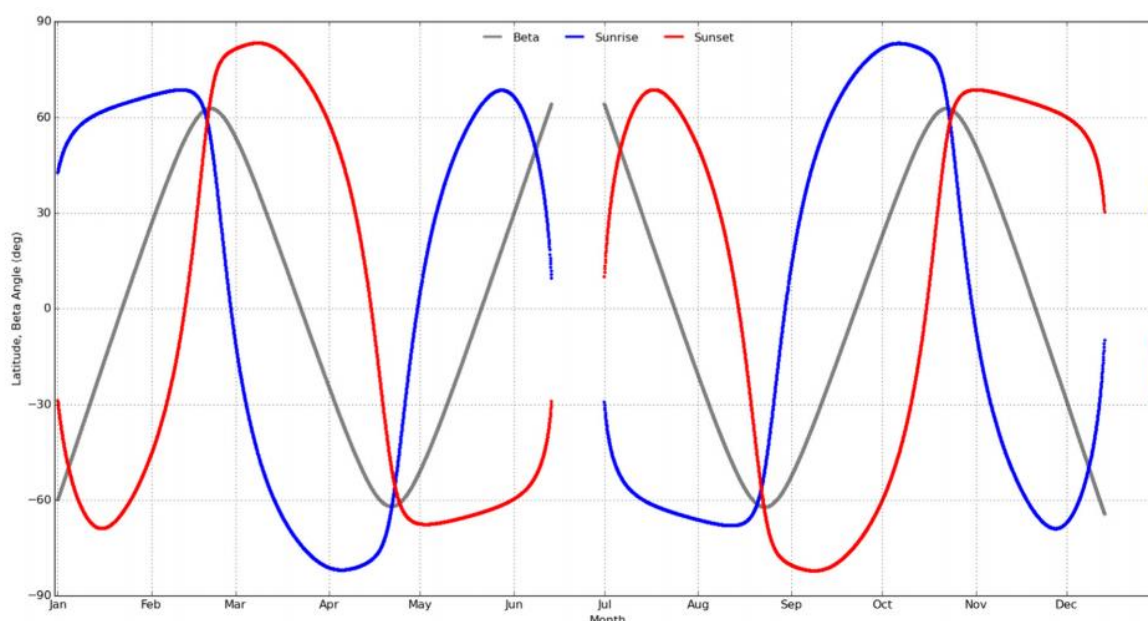


Figure 1. The latitude of ACE occultations for 1 year (2015) and the beta angle of the orbit

To maximise the number of matchups but reduce misinterpretation from setting the criteria too loosely, we looked for a coincidence of 300 km and 3 hours as a match. We use altitude as the vertical coordinate as this is the grid used by ACE, and also that there have been significant improvements in the MIPAS altitude assignment making altitude comparison, rather than pressure level comparisons, feasible. Values from the MIPAS have been interpolated onto the 1 km spacing of the ACE grid when a matchup occurs and data are presented on the 1 km vertical grid employed by ACE (generally 5.5 km, up to ~60.5 km for some species such as O<sub>3</sub>). The comparison approach largely follows that of Wetzel et al for the MIPAS balloon and satellite inter-comparisons and will be briefly detailed here.

Differences between measured quantities of MIPAS and ACE are expressed in absolute and relative units with the mean difference:

$$\Delta x_{mean} = \frac{1}{N} \sum_{n=1}^N (x_{M,n} - x_{A,n}) \quad (1)$$

where  $x_M$  and  $x_A$  are data values of MIPAS and ACE at one altitude level. The mean relative difference  $\Delta x_{mean,rel}$  of matching pairs is calculated by dividing through the mean absolute difference by the mean profile of the reference instrument, which is ACE:

$$\Delta x_{mean,rel} = \frac{\Delta x_{mean}}{\frac{1}{N} \sum_{n=1}^N x_{A,n}} \cdot 100\% \quad (2)$$

Differences are then displayed together with the combined errors  $\sigma_{comb}$  of both instruments, defined as:

$$\sigma_{comb} = \sqrt{\sigma_M^2 + \sigma_A^2} \quad (3)$$

where  $\sigma_M$  and  $\sigma_A$  are the precision, systematic or total errors of MIPAS. Errors from ACE are only given in terms of precision (and, inherently, this is also taken to be the total error).

Precision errors come mainly from the random noise errors on the retrieval. Systematic errors for MIPAS have been assessed in a corresponding study (Dudhia et al. (2002); Raspollini et al., 2013). The uncertainty of the calculated mean difference (standard error of the mean, SEM) is given by  $\frac{\sigma}{N^{0.5}}$  where  $\sigma$  is the standard deviation (SD) of the measurements. A bias between the instruments is significant if the SEM is smaller than the bias itself. The retrieval approach of ACE does not produce averaging kernels and so these cannot be applied to MIPAS data (and vice-versa) but the two instruments have a similar field of view of around 3-4 km.

### 3 Intercomparison results

In this section, we discuss the validation for a number of key species retrieved by the MIPAS operational L1v8/L2v8 processor based on collocated ACE observations. Gases include O3, HNO3, COF2, CCl4, HCN, C2H2, C2H6, CH3Cl, COCl2, HDO. MIPAS data used had to pass the a posteriori quality check (retrieval convergence and size of maximum error) to be used in the comparison. ACE data were similarly flagged and bad values and those which were simply the a priori assumptions were removed. Data are analysed globally although this is biased towards more data in the Northern and Southern Hemisphere mid-latitudes with virtually no data in the tropics (20S-20N) and few data at the poles (poleward of 65 degrees). Data are shown for each gas for each year between 2005 and 2012 for the version 4 ACE dataset.

Mean differences are shown by the red solid line, including the standard deviation (red dotted line) at each level alongside the standard error of the mean (SEM, plotted as error bars). The combined errors of MIPAS and ACE are shown in terms of precision (blue dotted lines) and total error (blue dashed lines, including systematic components where assessed). This is presented for absolute and relative terms.

ACE data were first produced operationally in January 2004, but given the issues with the MIPAS slide mirror in March of that year, we only consider the intercomparisons from January 2005 when the MIPAS began operations again after the new optimised resolution measurements began. An overview of the comparison is given in Table 3.

### 3.1 Ozone (O<sub>3</sub>)

Monitoring recovery of the ozone layer after the implementation of the Montreal Protocol is a key aim of MIPAS data products. Collocation comparisons, Figure 2, show an agreement between the satellites within  $\pm 10\%$  between 15 and 40 km for this mainly stratospheric species. For much of the stratosphere (15-40 km) the agreement is within  $\pm 5\%$  with very little variability across the different years pointing to a very stable and consistent product. A lower agreement is found in the upper troposphere and lower stratosphere (10-15 km) with differences up to  $\pm 30\%$ . Below 10 km the differences can be over 100%, but this is also the range of altitudes where some of the lowest VMRs occur.

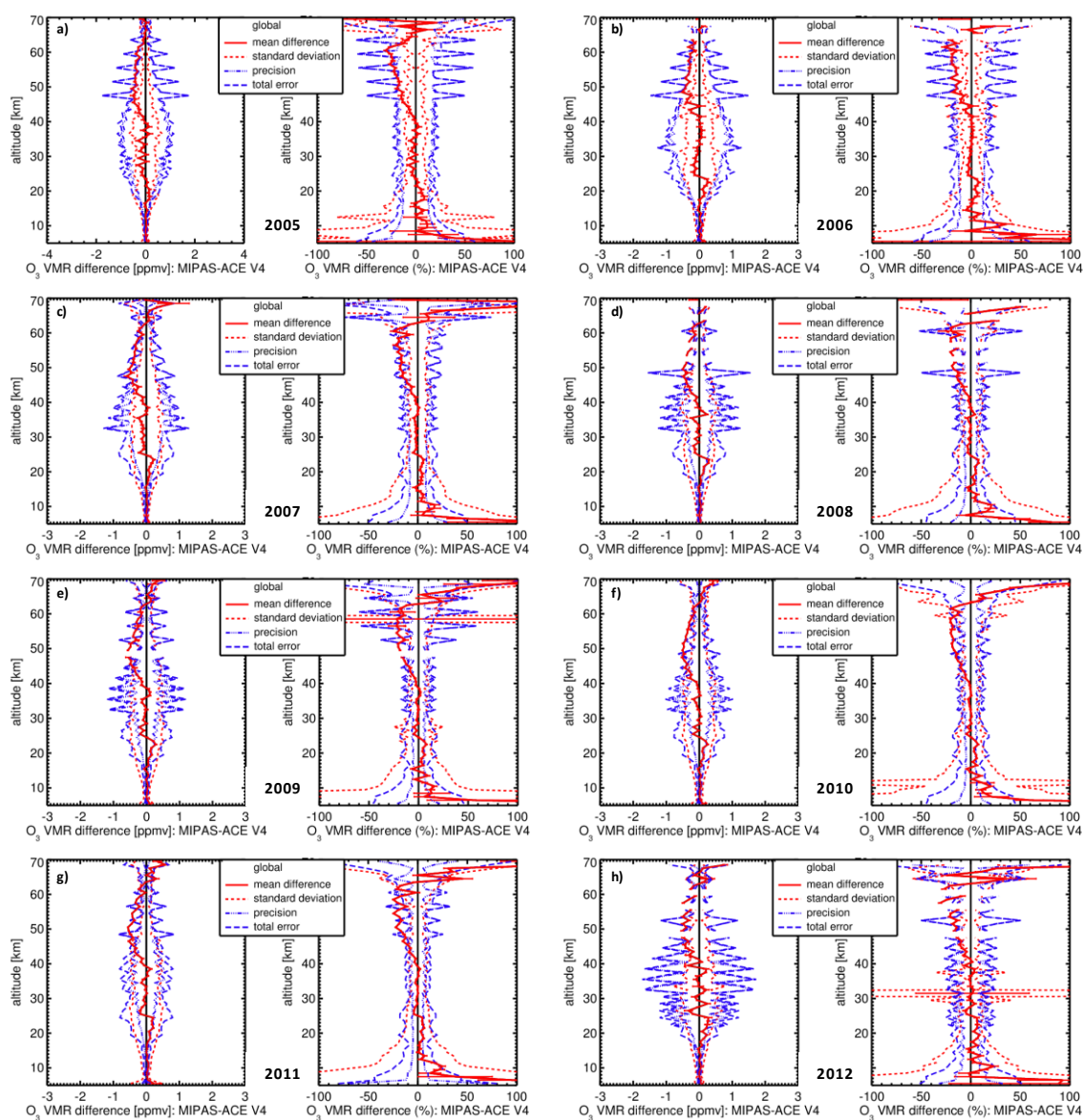


Figure 2. Mean absolute and relative O<sub>3</sub> VMR difference of all trajectory match collocation (red numbers) between MIPAS and ACE version 4 data (red solid line) including standard deviation (red dotted lines) and standard error of the mean



(plotted as error bars). Precision (blue dotted lines) and total (blue dashed lines) mean combined errors are shown, too. Global matchups. a) 2005, b) 2006, c) 2007, d) 2008, e) 2009, f) 2010 g) 2011, h) 2012. For details, see text.

### 3.2 Nitric Acid ( $\text{HNO}_3$ )

$\text{HNO}_3$  acts as a stratospheric nitrogen reservoir and the profile differences are seen in Figure 3. In the upper troposphere/lowermost stratosphere (12 km to 17 km) differences between the satellites are within  $\pm 10\%$ . In the lower stratosphere (17 km to 25 km) MIPAS is generally higher than ACE by up to 10%. By the upper stratosphere (25 km to 40 km) MIPAS is generally between 10%-30% lower than the ACE values. Overall, biases are typically in the order of 5-20% in relative units and in line with the numbers reported by Wang et al. (2007) referring to the FR period. Standard deviations exceed the expected total error.

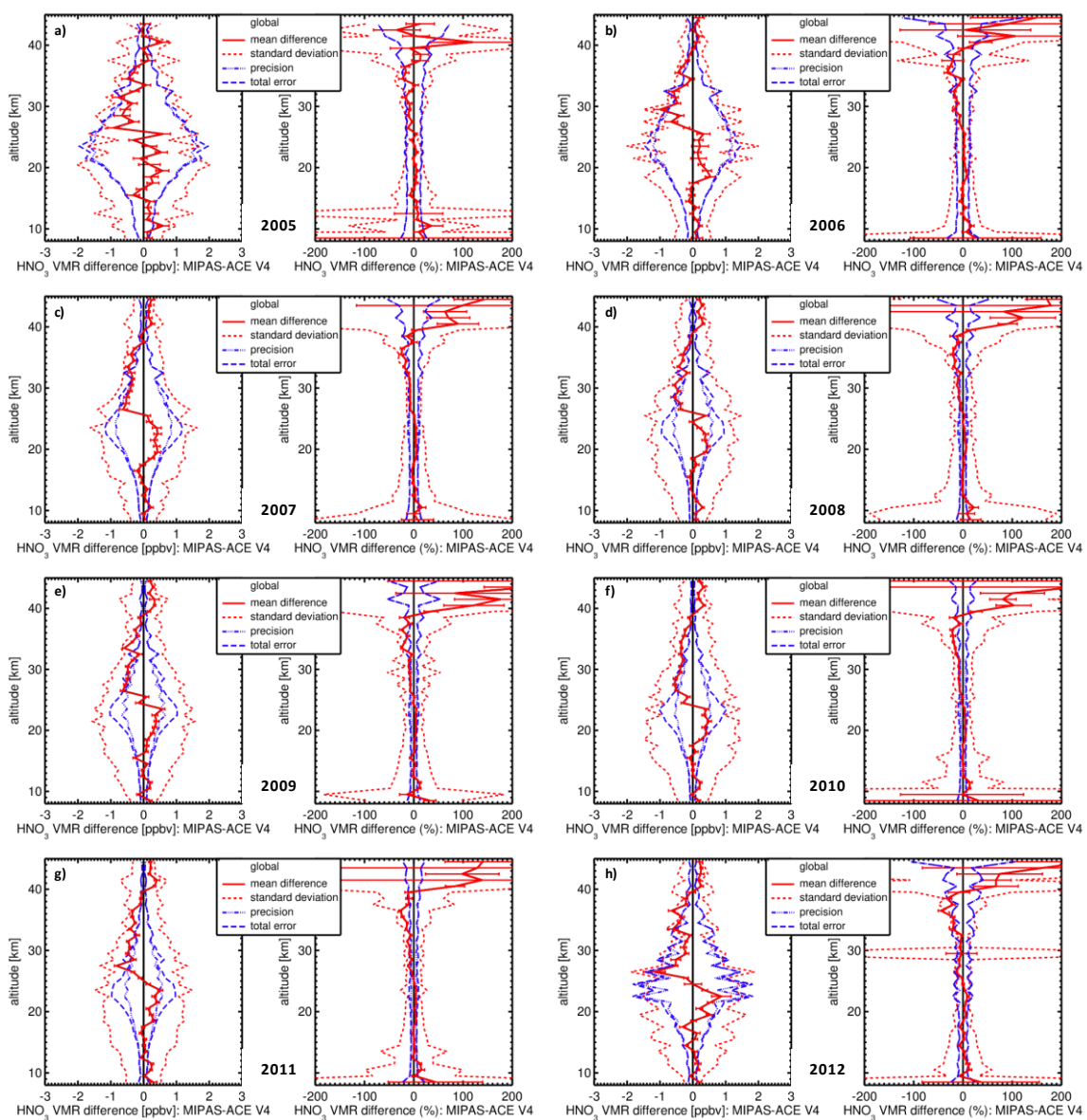


Figure 3. As Figure 2 but for  $\text{HNO}_3$ .

### 3.3 Carbonyl Fluoride (COF<sub>2</sub>)

Carbonyl fluoride acts as a reservoir species for fluorine, first introduced in version 8 MIPAS data, and profile shapes are generally consistent between MIPAS and ACE. VMR differences are smallest in the 15-18 km range across all years ( $\pm 10\%$ ). Above 18 km to the upper stratosphere (35 km) MIPAS is generally higher than ACE by between 20-40% across all years between 2005 and 2012. Above 20 km the differences exceed the expected total error on the differences, but it must be remembered that the ACE data contain no systematic error estimate for COF<sub>2</sub>.

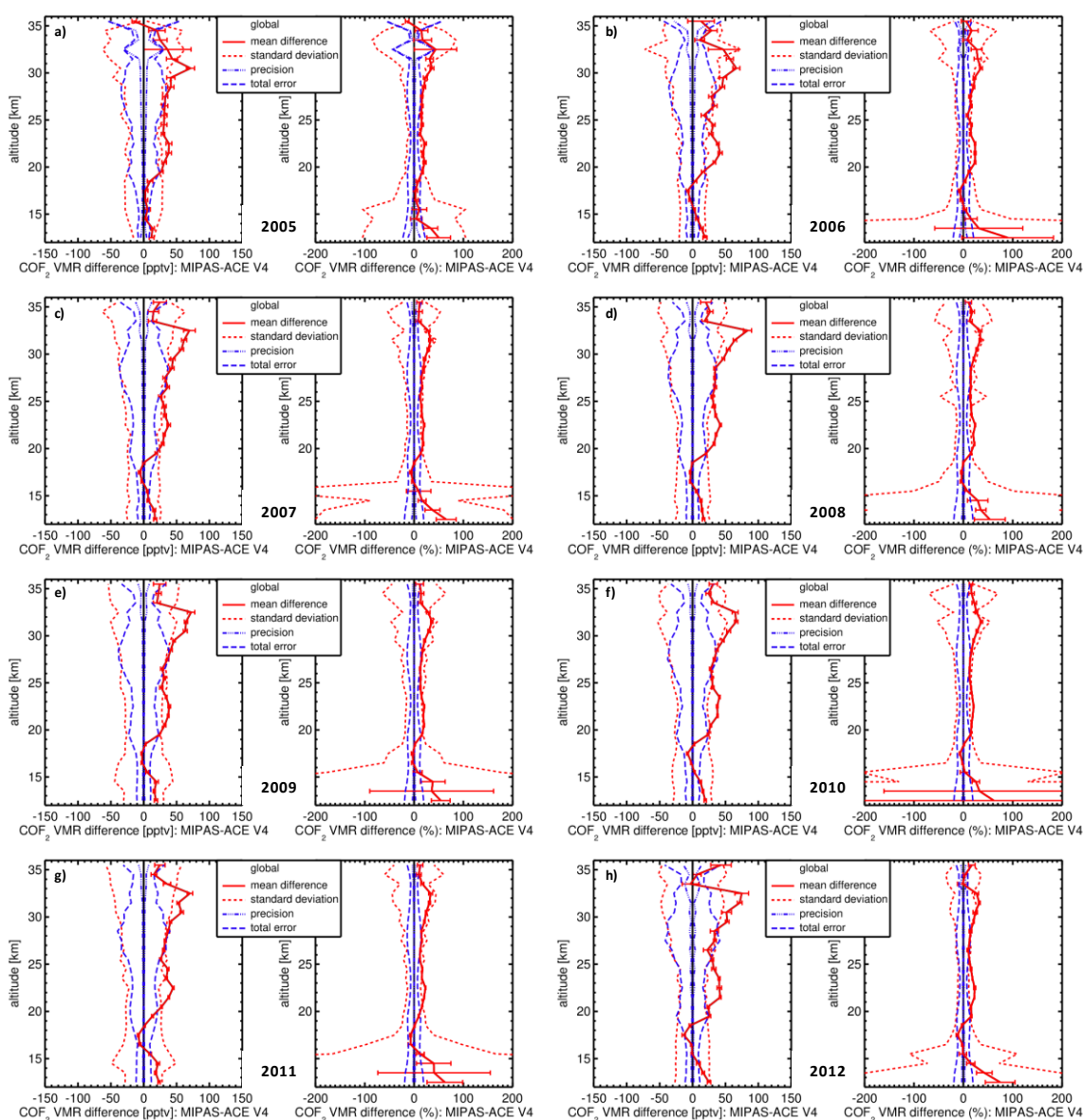


Figure 4. As Figure 2, but for COF<sub>2</sub>.



### 3.4 Carbon Tetrachloride (CCl<sub>4</sub>)

Carbon tetrachloride was first introduced in the v7 MIPAS data and its relevance is an ozone-depleting substance, accounting for about 10% of the chlorine in the troposphere. Despite being controlled by the Montreal Protocol, CCl<sub>4</sub> emissions from regions such as Eastern China showed no decline between 2009 and 2016 (Lunt et al. 2018). Estimated sources and sinks are generally inconsistent with observations of its abundance. From Figure 5, it can be seen that the best consistency between MIPAS and ACE observations is between 15 and 21 km for each year where the differences are between  $\pm 10\%$ . There is a significant negative bias above 22 km of up to 100%, which is in some cases outside the total error. Below 15 km MIPAS VMRs are generally higher than ACE by between 5% and 40%.

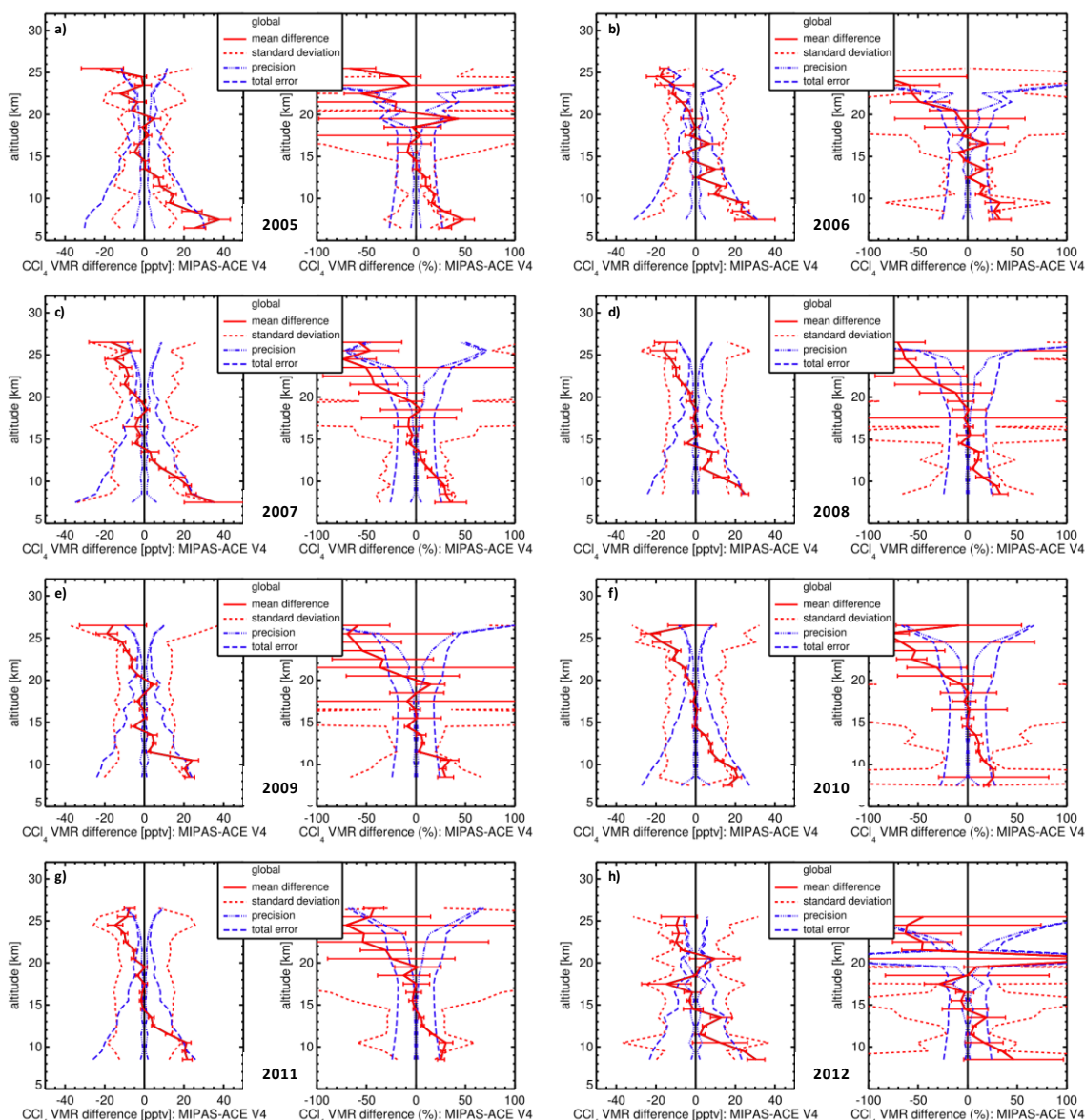


Figure 5. As Figure 2 but for CCl<sub>4</sub>.

### 3.5 Hydrogen Cyanide (HCN)

Hydrogen cyanide is a good marker of biomass burning and is often used by ACE to determine whether an air parcel has been affected recently by biomass burning (Tereszchuk et al. 2013). A significant positive bias is seen in the MIPAS data between 16 and 19 km of up to 100%, exceeding the total error, and observed across all years in the 2005 to 2012 range. Better consistency between 10% to 30% is observed between 9 and 15 km, where most of the elevated plumes of HCN occur after biomass burning events. Between 20 km and 23 km MIPAS VMRs are between 30% and 60% lower.

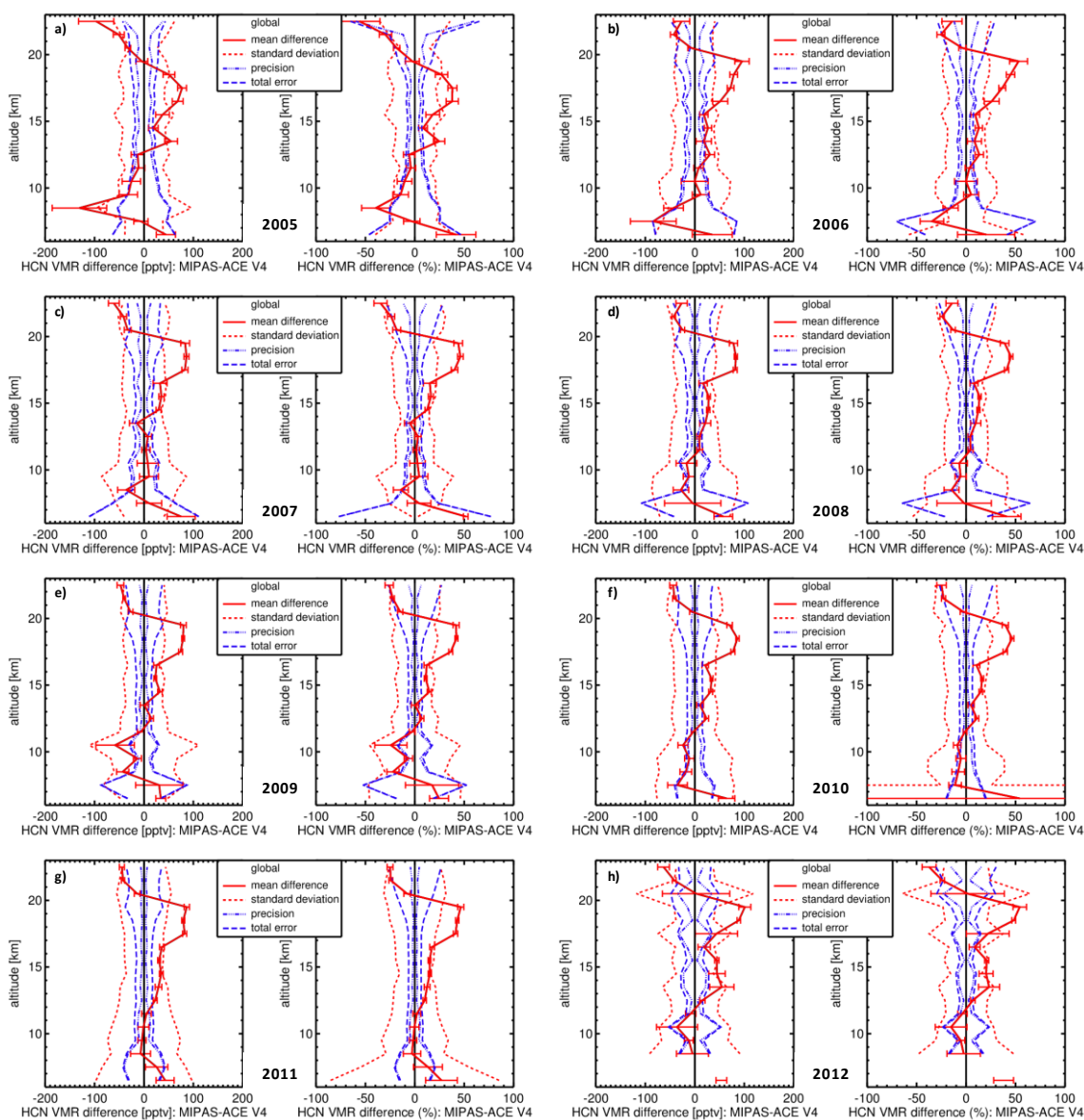


Figure 6. As Figure 2 but for HCN.

### 3.6 Acetylene (C<sub>2</sub>H<sub>2</sub>)

Acetylene is produced by both biomass burning and biofuel burning (Parker et al. 2011). The MIPAS VMRs are 10% to 50% lower than ACE across the profile (5 km to 25 km) and all years between 2005 and 2012, but within the expected total error. There are quite a few instances, particularly in the polar winters, where the C<sub>2</sub>H<sub>2</sub> signal gives many negative values which means that some care needs to be taken with the data for scientific needs.

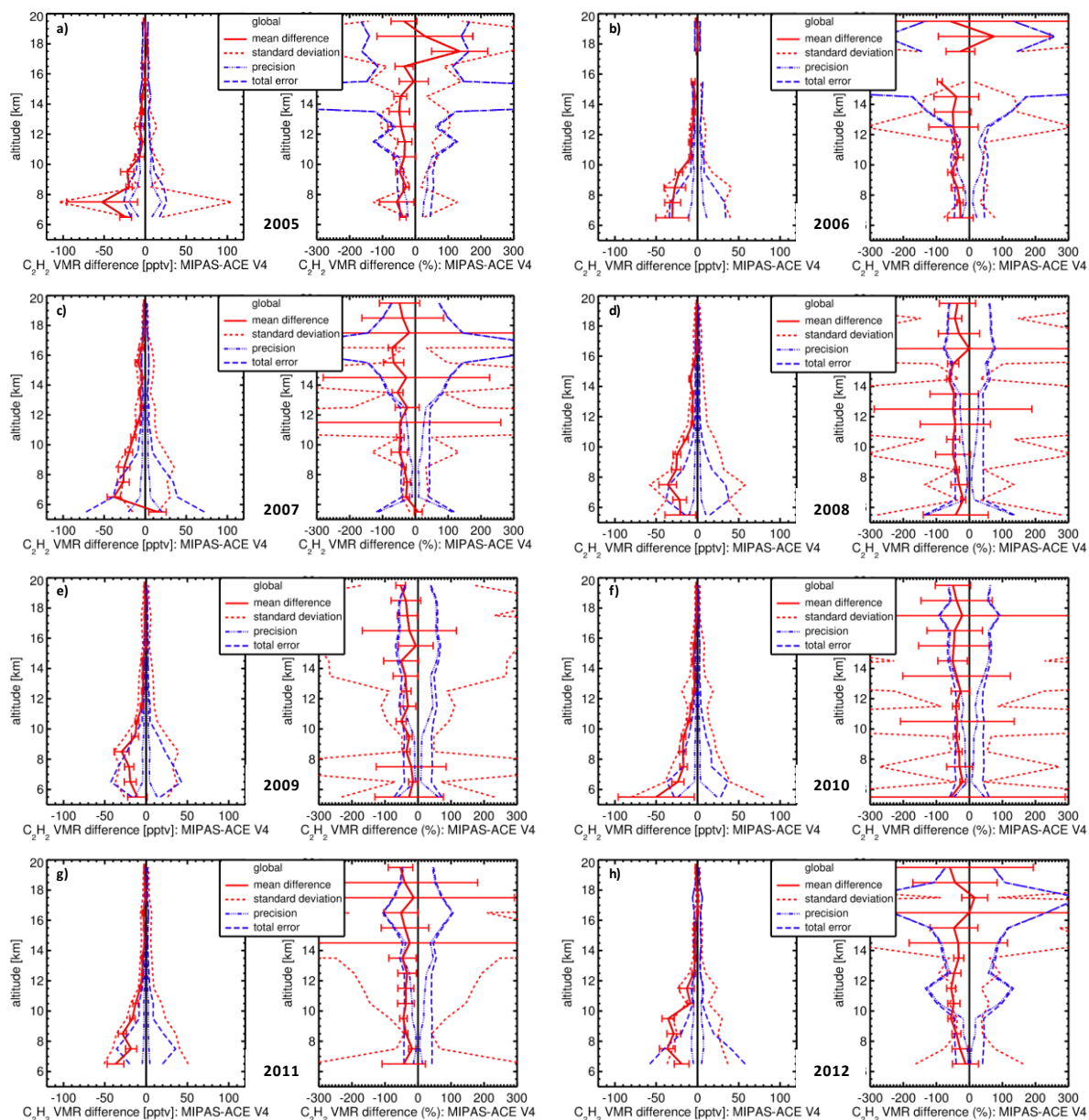


Figure 7. As Figure 2 but for C<sub>2</sub>H<sub>2</sub>.

### 3.7 Ethane (C<sub>2</sub>H<sub>6</sub>)

Ethane is produced from a variety of sources including biomass burning and fugitive emissions from fossil fuel burning. In the mid- to upper troposphere (6 km to 10 km) MIPAS ethane is between 30% and 50% higher than ACE, reducing to 20%-30% higher between 12 km and 14 km. Above 15 km, there is a much larger spread in the differences, which may be related to issues with ACE data at higher altitude, first reported for version 3.5/3.6. For version 4 ACE data, there were significant updates to the spectroscopy, updating from the HITRAN 2004 database to Harrison et al. 2010 and also a change in the set of microwindows used (Table 1). Version 4 of ACE is still awaiting validation so the results of the inter-comparison should be treated with caution at this stage.

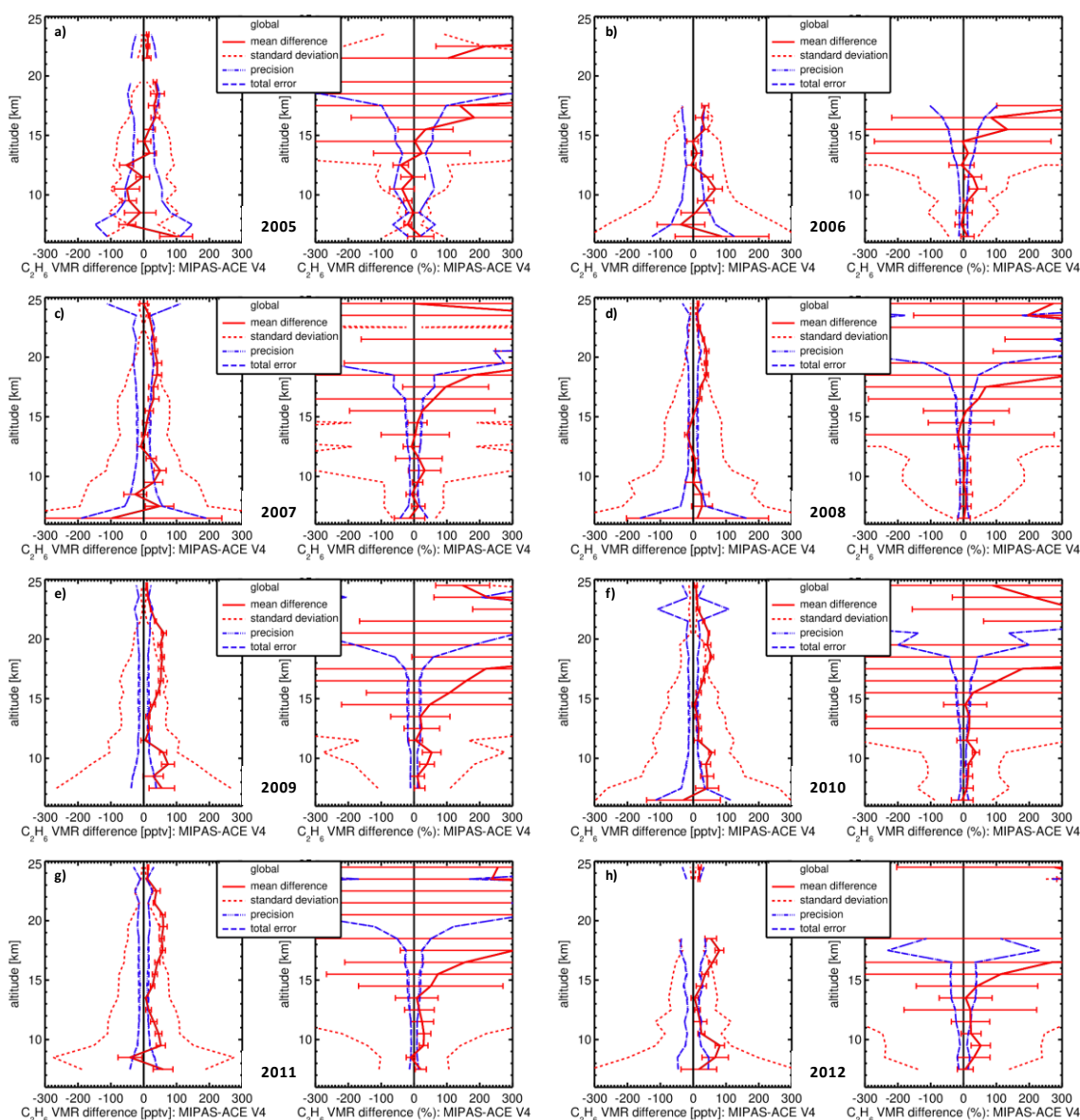


Figure 8. As Figure 2 but for C<sub>2</sub>H<sub>6</sub>.

Centre Frequency (cm <sup>-1</sup> )	Microwindow Width (cm <sup>-1</sup> )	Lower Altitude (km)	Upper Altitude (km)
1950.10 <sup>[1]</sup>	0.35	6-7	20
1977.60 <sup>[2]</sup>	0.50	6-7	20
2976.50	2.00	6-7	20

<sup>[1]</sup> Included to improve results for interferer H<sub>2</sub>O

<sup>[2]</sup> Included to improve results for interferer H<sub>2</sub>O isotopologue 2 (H<sup>18</sup>OH)

Centre Frequency (cm <sup>-1</sup> )	Microwindow Width (cm <sup>-1</sup> )	Lower Altitude (km)	Upper Altitude (km)
1950.10 <sup>[1]</sup>	0.35	6-7	20
1977.60 <sup>[2]</sup>	0.50	6-7	20
2976.55	0.90	5	30
2983.37	0.70	9-14	30
2986.55	0.70	5	30
2993.45	0.90	10-15	30
2996.60	1.20	5	30

<sup>[1]</sup> Included to improve results for interferer H<sub>2</sub>O

<sup>[2]</sup> Included to improve results for interferer H<sub>2</sub>O isotopologue 2 (H<sup>18</sup>OH)

Table 1. Microwindows used by the ACE C<sub>2</sub>H<sub>6</sub> retrieval for v3.5/3.6 (top) and v4 (bottom) retrievals.

### 3.8 Chloromethane (CH<sub>3</sub>Cl)

Chloromethane is the most abundant halocarbon in the atmosphere and is emitted from natural and anthropogenic sources (Yokouchi et al., 2000). Figure 9 shows that between 10 and 22 km there is a negative bias of within 5% to 50%. In the mid-stratosphere (22 km to 29 km) the differences stay within  $\pm 30\%$  but with a very large spread due to low VMRs. Above 29 km, there is significant negative bias of up to 100%.

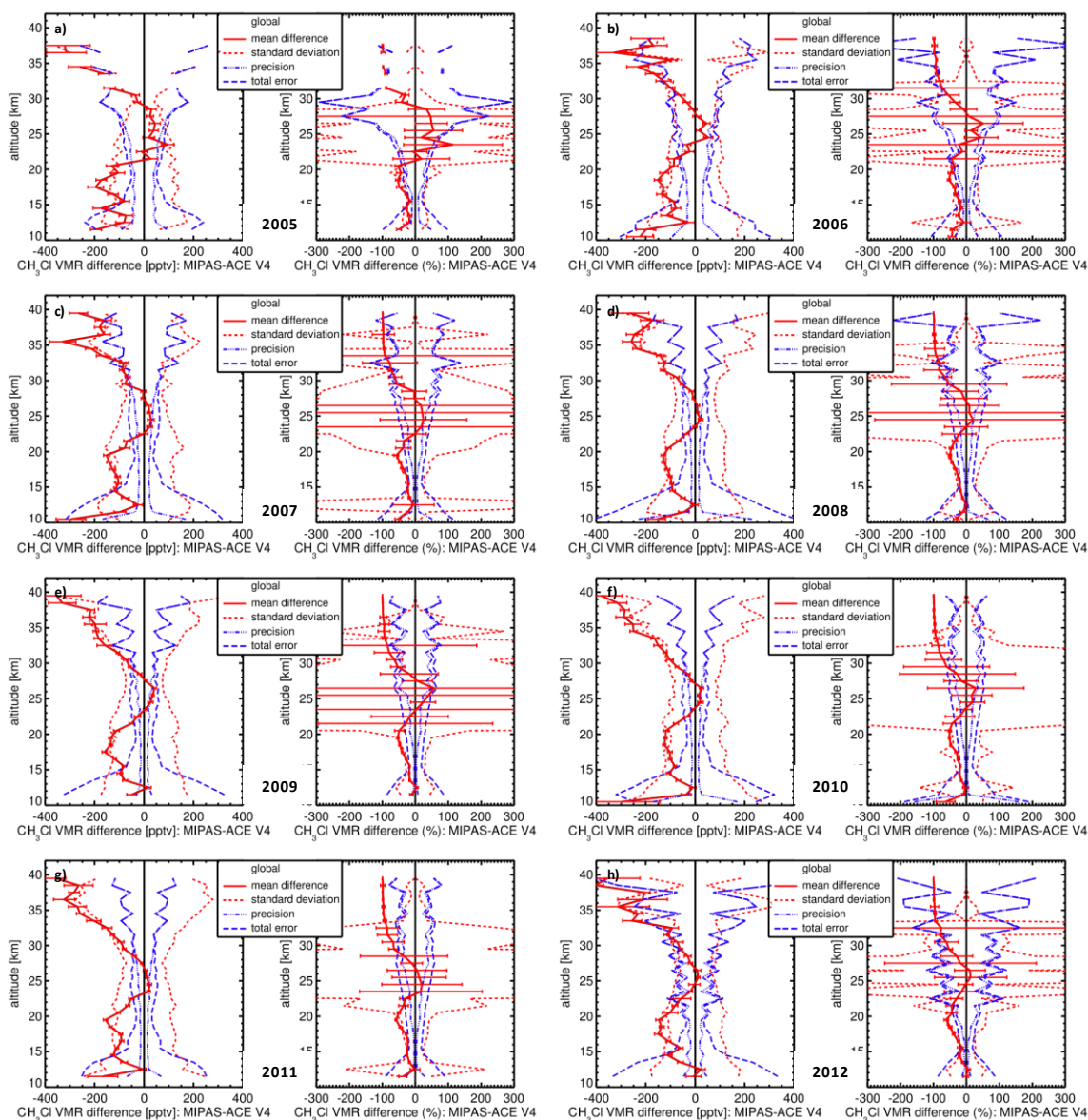


Figure 9. As Figure 2 but for CH<sub>3</sub>Cl.



### 3.9 Phosgene (COCl<sub>2</sub>)

Phosgene (COCl<sub>2</sub>) is a by-product of chemical industries and by OH-initiated oxidation of chlorinated hydrocarbons in the troposphere (Kindler et al., 1995; Fu et al., 2007; Valeri et al., 2016). Figure 10 shows that there is a very significant positive bias throughout the retrieved profiles between 8 km and 25 km of between 80% and 200%. There were very significant changes to the ACE COCl<sub>2</sub> product between the v3.5 and v4, most significantly the spectroscopy data was updated from the ATMOS linelist (Brown et al., 1995) to HITRAN 2016. Significant changes were also made to the microwindow list (Table 2) including many more lines in the 829 cm<sup>-1</sup> to 861.50 cm<sup>-1</sup> range. ACE COCl<sub>2</sub> has not yet been validated so comparisons should be viewed with some caution. For comparison, the results of the validation between MIPAS and ACE (v3.6) are shown in Figure 11. The profiles are now much more consistent with differences within ±30% throughout the 8 km to 25 km range.

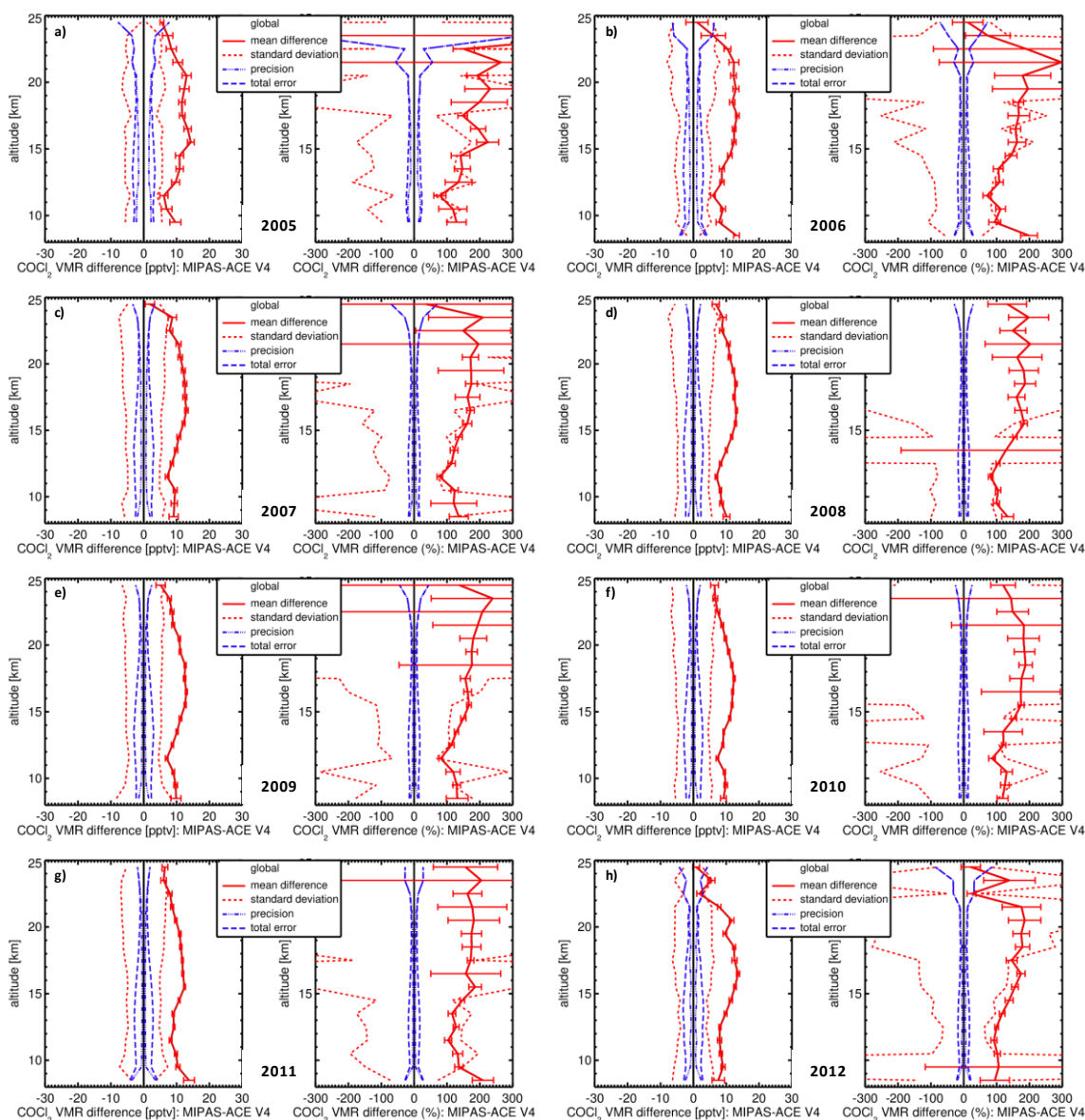


Figure 10. As Figure 2 but for COCl<sub>2</sub>.

Table 2. Microwindows used by the ACE COCl<sub>2</sub> retrieval for v3.5/3.6 (top) and v4 (bottom) retrievals.

Centre Frequency (cm <sup>-1</sup> )	Microwindow Width (cm <sup>-1</sup> )	Lower Altitude (km)	Upper Altitude (km)
844.00	28.00	8-10	23.5-28.5
1970.12 <sup>[1]</sup>	0.35	10	23.5-28.5
1977.60 <sup>[2]</sup>	0.50	8-10	21
2976.50 <sup>[3]</sup>	2.00	8-10	20

<sup>[1]</sup> Included to improve results for interferer CO<sub>2</sub>

<sup>[2]</sup> Included to improve results for interferer H<sub>2</sub>O isotopologue 2 (H<sup>18</sup>OH)

<sup>[3]</sup> Included to improve results for interferer C<sub>2</sub>H<sub>6</sub>

Centre Frequency (cm <sup>-1</sup> )	Microwindow Width (cm <sup>-1</sup> )	Lower Altitude (km)	Upper Altitude (km)
829.03	0.50	8-11	24-29
832.50	0.50	8-11	24-29
837.00	1.80	8-11	24-29
838.55	0.70	8-11	24-29
845.25	5.50	8-11	24-29
849.00	2.00	8-11	24-29
851.00	2.00	8-11	24-49
854.50	3.00	11-14	24-29
857.00	2.00	8-11	24-29
861.50	3.00	8-11	24-29
2976.50 <sup>[1]</sup>	2.00	8-11	20

<sup>[1]</sup> Included to improve results for interferer C<sub>2</sub>H<sub>6</sub>

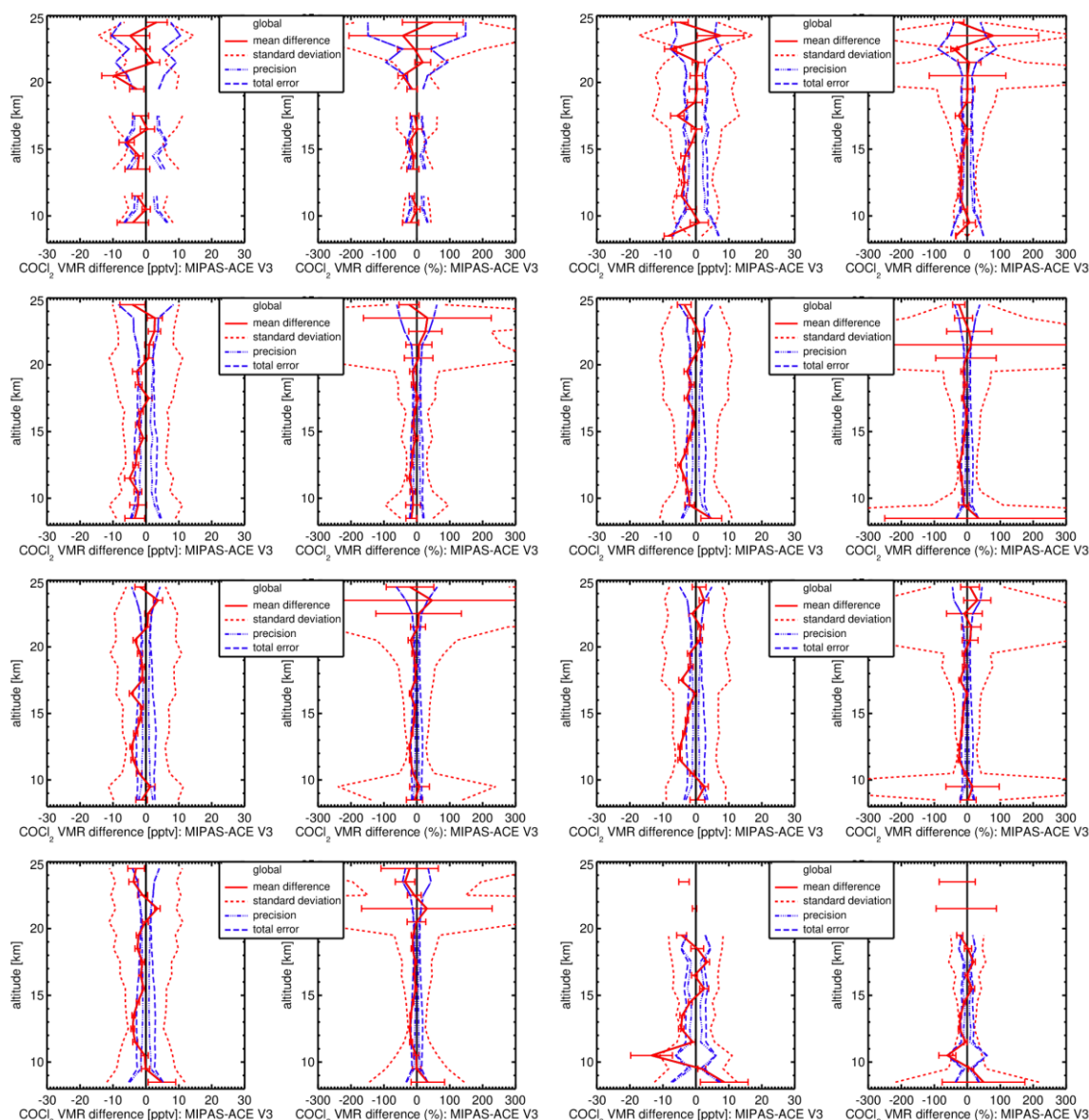


Figure 11. As Figure 2 but for COCl<sub>2</sub> and using the ACE v35/3.6 dataset.

### 3.10 Heavy Water (HDO)

The isotopic composition of water vapour provides unique information about convective processes and transport in the atmosphere. As water vapour condenses to liquid or ice, the heavier isotopologues, such as HDO, are preferentially removed in the vapour phase. Evaporating ice can carry the more enhanced isotopic signature of lower altitudes (Randel et al, 2012). Between 13 and 35 km the agreement between MIPAS and ACE is better than  $\pm 20\%$  and generally better than  $\pm 10\%$  in the stratosphere (18 km to 35 km). Above 35 km and up to 45 km, MIPAS is negatively biased by between 10% and 40%. Below 13 km, it is clear that negative bias of 10% to 50% occurs.

Alongside the ESA L1v8/L2v8 full mission data, an improved HDO research product from the KIT group is under development (M. Kiefer, pers. Comms.) and referred to hereafter as HDO-KIT. Previous versions of the product are outlined in the validation paper by Lossow et al., 2011. To assess the quality of HDO-KIT Lossow et al., 2011, made their own comparisons to ACE-FTS satellite data alongside measurements made by the Odin/SMR satellite. The authors found the largest differences to ACE-FTS below 15 km where relative deviations occasionally exceeded 100%. Above 20 km, they found very good consistency between HDO-KIT/ACE/SMR, with MIPAS and ACE agreement to within 10% with HDO-KIT showing higher abundances than ACE-FTS.

In this study we compare operational MIPAS HDO to ACE-SCISAT and, additionally, MIPAS HDO to a more recent, yet unpublished version of HDO-KIT by the profile-to-profile comparisons averaged over years. As we can compare to the whole 2002 to 2012 period of data for HDO-KIT we are also able to compare and contrast full-resolution and optimal resolution data periods. For operational MIPAS and HDO-KIT we also show regional differences due to the better global matchup coverage we are able to get. Regions shown are the Arctic ( $65^{\circ}\text{N}$ - $90^{\circ}\text{N}$ ), Northern Hemisphere mid-latitudes (nh\_midl  $20^{\circ}\text{N}$ - $65^{\circ}\text{N}$ ), the tropics ( $20^{\circ}\text{S}$ - $20^{\circ}\text{N}$ ), the Southern Hemisphere mid-latitude (sh\_midl  $20^{\circ}\text{S}$ - $65^{\circ}\text{S}$ ) and Antarctica ( $65^{\circ}\text{S}$ - $90^{\circ}\text{S}$ ).

For global MIPAS/ACE v4 comparisons, Figure 12, it was found that below 13 km, MIPAS is between 10% and 50% lower than ACE. Between 13 km and 35 km there is much greater consistency, between  $\pm 20\%$  and generally better than 10%. Above 35 km MIPAS is again lower than ACE by between 20% and 50%.

Comparisons of MIPAS operational product to HDO-KIT, Figure 13, yielded some very consistent and favourable results in the full-resolution data period (2002-2004). The best agreement between the two datasets overall was found to occur between the upper troposphere and the upper stratosphere (15 km to 50 km), within  $\pm 10\%$ , which was also reproduced across all latitude regions in the regional analysis, Figure 13. Globally, operational MIPAS was lower than HDO-KIT by between 5% and 40% and this was representative of all regions. Below 9 km there was more inconsistency with the global average showing operational MIPAS data could be up to as much as 150% high, particularly in the arctic and northern hemisphere mid-lats.

During the optimised resolution period (2005-2012) there was also good consistency between the operational MIPAS HDO and HDO-KIT, Figure 14. The highest consistency globally was between 15 km and 35 km, within  $\pm 15\%$ . This was also represented across the five regional latitude bands, although the tropics showed less consistency of between  $\pm 30\%$ . Below 15 km, MIPAS was between 10% and 100% lower than HDO-KIT. In the upper stratosphere (35 km to 50 km), MIPAS was lower by between 10%-30%. By the mesosphere (50 km to 65 km), MIPAS are higher by 10%-50%. Larger positive bias of MIPAS is found in the arctic mesosphere at up to 100%.

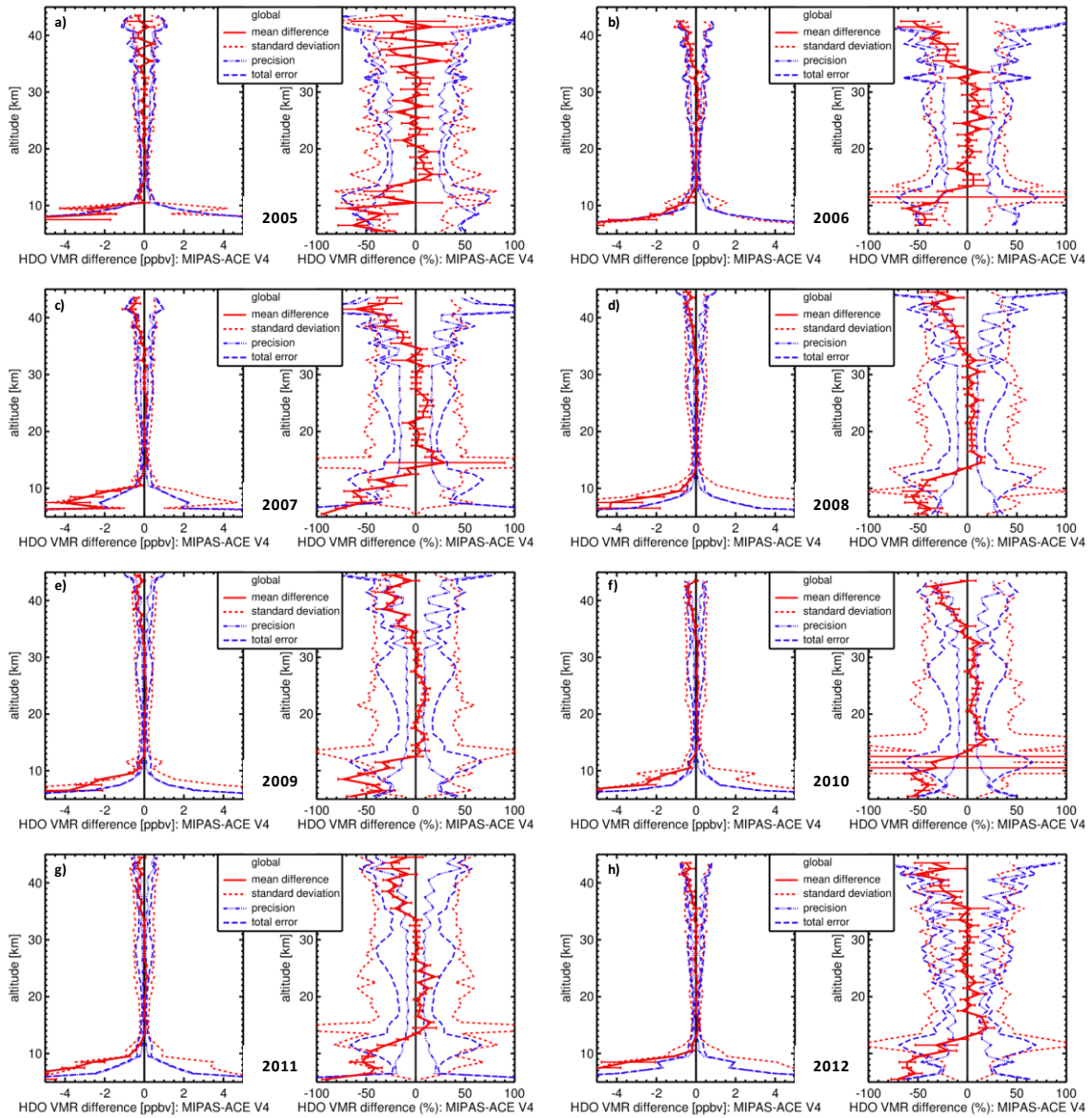


Figure 12. As Figure 2 but for HDO.

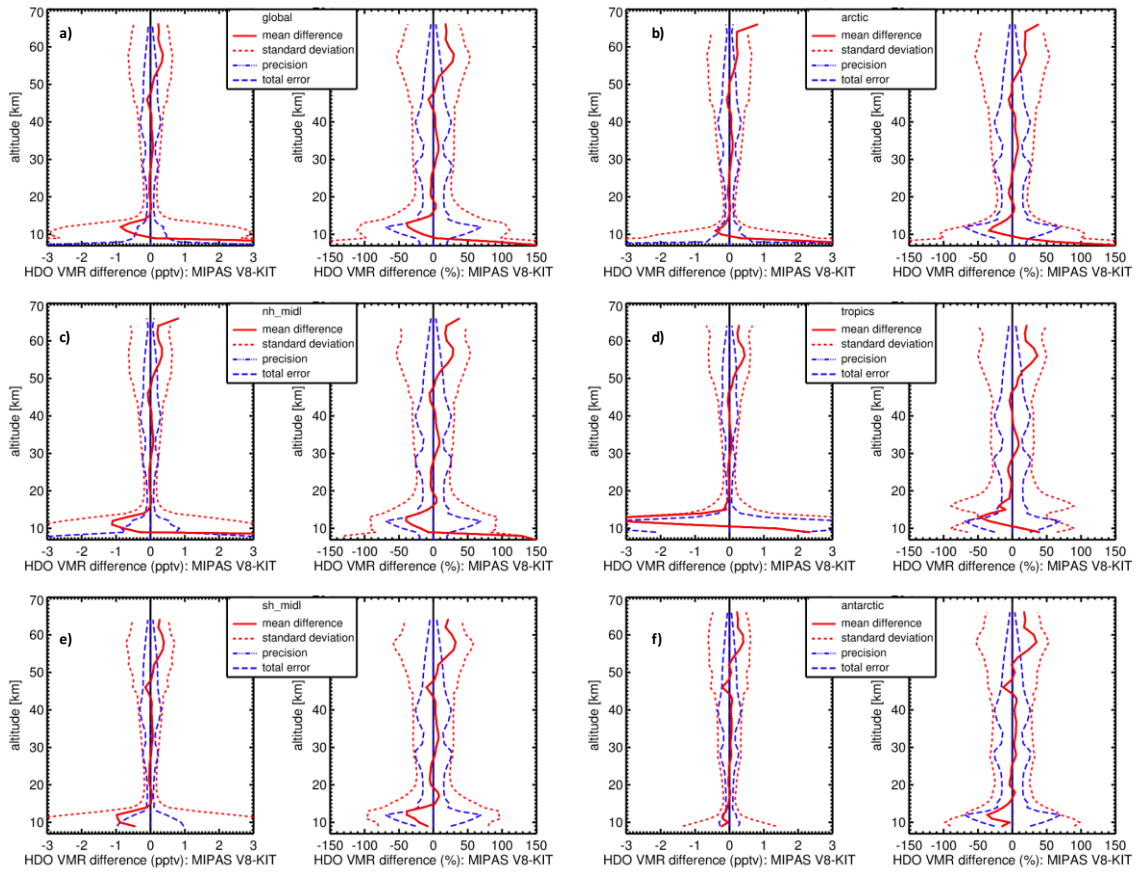


Figure 13. Mean absolute and relative HDO VMR difference of all match collocation (red numbers) between operational v8 MIPAS and KIT HDO data (red solid line) including standard deviation (red dotted lines) and standard error of the mean (plotted as error bars). Precision (blue dotted lines) and total (blue dashed lines) mean combined errors are shown, too for 2002-2004 during the MIPAS instrument full-resolution period. a) Global matchups, b) arctic [65N-90N], c) Northern Hemisphere mid-latitudes [20N-65N], d) tropics [20S-20N], e) Southern Hemisphere mid-latitudes [20S-65S], f) Antarctica [65S-90S]. For details, see text.



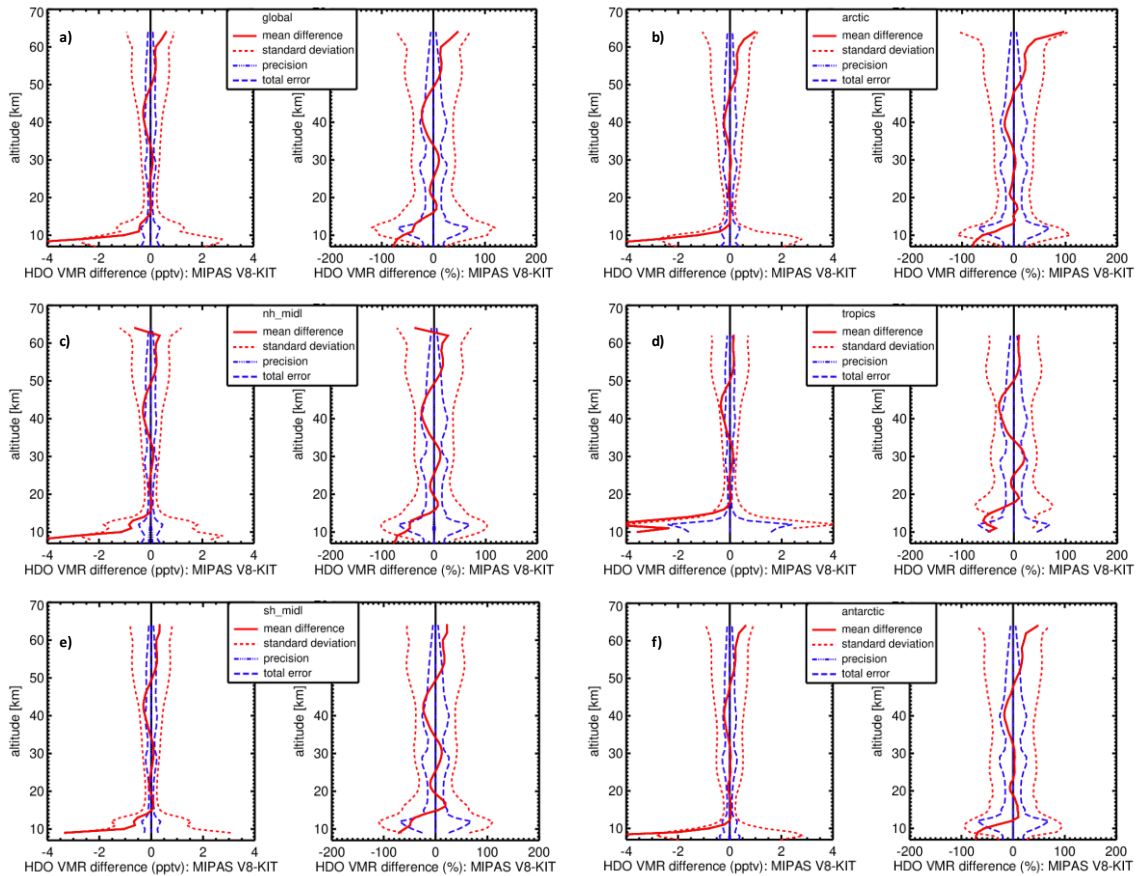


Figure 14. As Figure 13, but for 2005-2012.

Table 3. Summary of MIPAS validation results comparison to ACE-FTS on SCISAT. Mentioned atmospheric parameter differences refer to MIPAS minus the ACE-FTS instrument.

Parameter	Comments (L1v8/L2v8 FM)
$O_3$	Agreement $\pm 10\%$ 15 km to 40 km
$HNO_3$	Significant positive bias of more than 10% between 17 km to 25 km. MIPAS negative bias of between 10% and 30% between 25 km and 40km
$COF_2$	Significant positive bias between 20% and 40%
$CCl_4$	Significant negative bias above 22 km and significant positive bias below 15 km
$HCN$	Below 15 km, agreement within $\pm 30\%$ . A persistent positive artefact in the MIPAS data between 16 km and 19 km.
$C_2H_2$	Negative bias of between 5% and 50%
$C_2H_6$	Positive bias of between 20% and 50%
$CH_3Cl$	Agreement $\pm 30\%$ between 22 km and 29 km.
$COCl_2$	Significant positive offset in the MIPAS by between 80% and 200% in the profile
$HDO$	Excellent consistency with KIT HDO product of between $\pm 10\%$ between 15 km and 50 km. Consistency with ACE between 13 km and 35 km better than $\pm 20\%$



## 4 Conclusions

Vertical profiles of ACE-FTS solar occultation measurements between 2004 and 2012 have been used for an intercomparison study of some major gas retrieved by MIPAS and some of the new species retrieved in the version 8 of the operational MIPAS processor.

For some of the previously measured species ( $O_3$ ,  $HNO_3$ ,  $COF_2$ ,  $CCl_4$  and  $HCN$ ), there is excellent consistency between MIPAS and ACE-FTS, particularly  $O_3$  and  $HNO_3$ . These species are both consistent to within  $\pm 10\%$  with ACE-FTS in the stratosphere.  $COF_2$ ,  $CCl_4$  and  $HCN$  show biases in the results and caution is advised when these data are used for scientific studies.

Some of the new v8 species ( $C_2H_2$ ,  $C_2H_6$ ,  $COCl_2$  and  $CH_3Cl$ ) show some large deviations. Some negative values of  $C_2H_2$  and  $C_2H_6$  are found in the colder wintertime measurements.  $COCl_2$  shows a significant offset in the comparison to ACE v4 data, which didn't occur with the comparison to ACE v3.6 data, which should be investigated in future study.  $C_2H_2$ ,  $C_2H_6$  and  $CH_3Cl$  should be used with caution for scientific studies. Another new species,  $HDO$ , shows some excellent agreement to ACE-FTS throughout the stratosphere. The first intercomparisons between the operational MIPAS  $HDO$  and a research product from KIT yielded some excellent agreement in the stratosphere also.

## 5 References

Bernath, P.F.: The Atmospheric Chemistry Experiment (ACE), *J. Quant. Spectrosc. Rad. Transfer.*, 186, 3-16, 10.1016/j.jqsrt.2016.04.006, 2017.

Brown, L.R., Gunson, M.R., Toth, R.A., Irion, F.W., Rinsland, C.P., and Goldman A., 1995 Atmospheric Trace Molecule Spectroscopy (ATMOS) linelist, *Appl. Opt.*, 35, 2828-2848, doi: <https://doi.org/10.1364/AO.35.002828>, 1996.

Cortesi, U., Lambert, J. C., De Clercq, C., Bianchini, G., Blumenstock, T., Bracher, A., Castelli, E., Catoire, V., Chance, K. V., De Mazière, M., Demoulin, P., Godin-Beekmann, S., Jones, N., Jucks, K., Keim, C., Kerzenmacher, T., Kuellmann, H., Kuttippurath, J., Iarlori, M., Liu, G. Y., Liu, Y., McDermid, I. S., Meijer, Y. J., Mencaraglia, F., Mikuteit, S., Oelhaf, H., Piccolo, C., Pirre, M., Raspollini, P., Ravegnani, F., Reburn, W. J., Redaelli, G., Remedios, J. J., Sembhi, H., Smale, D., Steck, T., Taddei, A., Varotsos, C., Vigouroux, C., Waterfall, A., Wetzol, G., and Wood, S.: Geophysical validation of MIPAS-ENVISAT operational ozone data, *Atmos. Chem. Phys.*, 7, 4807-4867, doi:10.5194/acp-7-4807-2007, 2007.

Dudhia, A., Jay, V. L., and Rodgers, C.D.: Microwindow selection for high-spectral-resolution sounders, *Appl. Opt.* 41, 3665-3673, 2002, (<http://eodg.atm.ox.ac.uk/MIPAS/err/>).

ESA: ESA declares end of mission for ENVISAT, ESA news 9 May 2012, available at: [http://www.esa.int/esaCP/SEM1SXSWT1H\\_index\\_0.html](http://www.esa.int/esaCP/SEM1SXSWT1H_index_0.html), 2012.

Fischer, H. and Oelhaf, H.: Remote sensing of vertical profiles of atmospheric trace constituents with MIPAS limb emission spectrometers, *Appl. Optics*, 35, 2787-2796, <https://doi.org/10.1364/AO.35.002787>, 1996.

Fischer, H., Birk, M., Blom, C., Carli, B., Carlotti, M., von Clarmann, T., Delbouille, L., Dudhia, A., Ehhalt, D., Endemann, M., Flaud, J. M., Gessner, R., Kleinert, A., Koopman, R., Langen, J., López-Puertas, M., Mosner, P., Nett, H., Oelhaf, H., Perron, G., Remedios, J., Ridolfi, M., Stiller, G., and Zander, R.: MIPAS:

an instrument for atmospheric and climate research, *Atmos. Chem. Phys.*, 8, 2151-2188, doi:10.5194/acp-8-2151-2008, 2008.

Fu, D., Boone, C. D., Bernath, P. F., Walker, K. A., Nassar, R., Manney, G. L., and McLeod, S. D.: Global phosgene observations from the Atmospheric Chemistry Experiment (ACE) mission, *Geophys. Res. Lett.*, 34, L17815, doi:10.1029/2007GL029942, 2007.

Kindler, T. P., Chameides, W. L., Wine, P. H., Cunnold, D. M., Alyea, F. N., and Franklin, J. A.: The fate of atmospheric phosgene and the stratospheric chlorine loadings of its parent compounds: CCl<sub>4</sub>, C<sub>2</sub>Cl<sub>4</sub>, C<sub>2</sub>HCl<sub>3</sub>, CH<sub>3</sub>CCl<sub>3</sub>, and CHCl<sub>3</sub>, *J. Geophys. Res.-Atmos.*, 100, 1235–1251, doi:10.1029/94JD02518, 1995.

Lossow, S., Steinwagner, J., Urban, J., Dupuy, E., Boone, C. D., Kellmann, S., Linden, A., Kiefer, M., Grabowski, U., Glatthor, N., Höpfner, M., Röckmann, T., Murtagh, D. P., Walker, K. A., Bernath, P. F., von Clarmann, T., and Stiller, G. P.: Comparison of HDO measurements from Envisat/MIPAS with observations by Odin/SMR and SCISAT/ACE-FTS, *Atmos. Meas. Tech.*, 4, 1855–1874, <https://doi.org/10.5194/amt-4-1855-2011>, 2011.

Lunt, M. F.; Park, S.; Li, S.; Henne, S.; Manning, A. J.; Ganesan, A. L.; Simpson, I. J.; Blake, D. R.; Liang, Q.; O'Doherty, S. et al.: Continued Emissions of the Ozone-Depleting Substance Carbon Tetrachloride From Eastern Asia. *Geophys. Res. Lett.*, 45, 11423– 11430, DOI: 10.1029/2018GL079500, 2018.

Parker, R. J., Remedios, J. J., Moore, D. P., and Kanawade, V. P.: Acetylene C<sub>2</sub>H<sub>2</sub> retrievals from MIPAS data and regions of enhanced upper tropospheric concentrations in August 2003, *Atmos. Chem. Phys.*, 11, 10243-10257, doi:10.5194/acp-11-10243-2011, 2011.

Payan, S., Camy-Peyret, C., Oelhaf, H., Wetzel, G., Maucher, G., Keim, C., Pirre, M., Huret, N., Engel, A., Volk, M. C., Kuellmann, H., Kuttippurath, J., Cortesi, U., Bianchini, G., Mencaraglia, F., Raspollini, P., Redaelli, G., Vigouroux, C., De Mazière, M., Mikuteit, S., Blumenstock, T., Velazco, V., Notholt, J., Mahieu, E., Duchatelet, P., Smale, D., Wood, S., Jones, N., Piccolo, C., Payne, V., Bracher, A., Glatthor, N., Stiller, G., Grunow, K., Jeseck, P., Te, Y., and Butz, A.: Validation of version- 4.61 methane and nitrous oxide observed by MIPAS, *Atmos. Chem. Phys.*, 9, 413-442, doi:10.5194/acp-9-413-2009, 2009.

Randel, W. J., Moyer, E., Park, M., Jensen, E., Bernath, P., Walker, K., and Boone, C.: Global variations of HDO and HDO/H<sub>2</sub>O ratios in the upper troposphere and lower stratosphere derived from ACE-FTS satellite measurements, *J. Geophys. Res.-Atmos.*, 117, D06303, <https://doi.org/10.1029/2011jd016632>, 2012.

Raspollini, P., Belotti, C., Burgess, A., Carli, B., Carlotti, M., Ceccherini, S., Dinelli, B. M., Dudhia, A., Flaud, J.-M., Funke, B., Höpfner, M., López-Puertas, M., Payne, V., Piccolo, C., Remedios, J. J., Ridolfi, M., and Spang, R.: MIPAS level 2 operational analysis, *Atmos. Chem. Phys.*, 6, 5605–5630, doi:10.5194/acp-6-5605-2006, 2006.

Raspollini, P., Carli, B., Carlotti, M., Ceccherini, S., Dehn, A., Dinelli, B. M., Dudhia, A., Flaud, J.-M., López-Puertas, M., Niro, F., Remedios, J. J., Ridolfi, M., Sembhi, H., Sgheri, L., and von Clarmann, T.: Ten years of MIPAS measurements with ESA Level 2 processor V6 – Part 1: Retrieval algorithm and diagnostics of the products, *Atmos. Meas. Tech.*, 6, 2419-2439, doi:10.5194/amt-6-2419-2013, 2013.

Ridolfi, M., Carli, B., Carlotti, M., von Clarmann, T., Dinelli, B. M., Dudhia, A., Flaud, J.-M., Höpfner, M., Morris, P. E., Raspollini, P., Stiller, G., and Wells, R. J.: Optimized forward model and retrieval scheme for MIPAS near-real-time data processing, *Appl. Opt.*, 39, 1323–1340, 2000.

Ridolfi, M., Blum, U., Carli, B., Catoire, V., Ceccherini, S., Claude, H., De Clercq, C., Fricke, K. H., Friedl-Vallon, F., Iarlori, M., Keckhut, P., Kerridge, B., Lambert, J.-C., Meijer, Y. J., Mona, L., Oelhaf, H., Pappalardo, G., Pirre, M., Rizi, V., Robert, C., Swart, D., von Clarmann, T., Waterfall, A., and Wetzel, G.: Geophysical validation of temperature retrieved by the ESA processor from MIPAS/ENVISAT atmospheric limb emission measurements, *Atmos. Chem. Phys.*, 7, 4459-4487, doi:10.5194/acp-7-4459-2007, 2007.

Stiller, G. P.: The Karlsruhe optimized and precise radiative transfer algorithm (KOPRA), Tech. rep., Wissenschaftliche Berichte FZKA 6487, 2000.

Terezschuk, K. A., Moore, D. P., Harrison, J. J., Boone, C. D., Park, M., Remedios, J. J., Randel, W. J., and Bernath, P. F.: Observations of peroxyacetyl nitrate (PAN) in the upper troposphere by the Atmospheric Chemistry Experiment-Fourier Transform Spectrometer (ACE-FTS), *Atmos. Chem. Phys.*, 13, 5601–5613, <https://doi.org/10.5194/acp-13-5601-2013>, 2013.

Valeri, M., Barbara, F., Boone, C., Ceccherini, S., Gai, M., Maucher, G., Raspollini, P., Ridolfi, M., Sgheri, L., Wetzel, G., and Zoppetti, N.: CCl<sub>4</sub> distribution derived from MIPAS ESA v7 data: intercomparisons, trend, and lifetime estimation, *Atmos. Chem. Phys.*, 17, 10143- 10162, doi:10.5194/acp-17-10143-2017, 2017.

Wang, D. Y., Höpfner, M., Blom, C. E., Ward, W. E., Fischer, H., Blumenstock, T., Hase, F., Keim, C., Liu, G. Y., Mikuteit, S., Oelhaf, H., Wetzel, G., Cortesi, U., Mencaraglia, F., Bianchini, G., Redaelli, G., Pirre, M., Catoire, V., Huret, N., Vigouroux, C., De Mazière, M., Mahieu, E., Demoulin, P., Wood, S., Smale, D., Jones, N., Nakajima, H., Sugita, T., Urban, J., Murtagh, D., Boone, C. D., Bernath, P. F., Walker, K. A., Kuttippurath, J., Kleinböhl, A., Toon, G., and Piccolo, C.: Validation of MIPAS HNO<sub>3</sub> operational data, *Atmos. Chem. Phys.*, 7, 4905-4934, doi:10.5194/acp-7-4905-2007, 2007.

Wetzel, G., Bracher, A., Funke, B., Goutail, F., Hendrick, F., Lambert, J.-C., Mikuteit, S., Piccolo, C., Pirre, M., Bazureau, A., Belotti, C., Blumenstock, T., De Mazière, M., Fischer, H., Huret, N., Ionov, D., López-Puertas, M., Maucher, G., Oelhaf, H., Pommereau, J.-P., Ruhnke, R., Sinnhuber, M., Stiller, G., Van Roozendaal, M., and Zhang, G.: Validation of MIPAS-ENVISAT NO<sub>2</sub> operational data, *Atmos. Chem. Phys.*, 7, 3261-3284, doi:10.5194/acp-7-3261-2007, 2007.

Wetzel, G., Oelhaf, H., Berthet, G., Bracher, A., Cornacchia, C., Feist, D. G., Fischer, H., Fix, A., Iarlori, M., Kleinert, A., Lengel, A., Milz, M., Mona, L., Müller, S. C., Ovarlez, J., Pappalardo, G., Piccolo, C., Raspollini, P., Renard, J.-B., Rizi, V., Rohs, S., Schiller, C., Stiller, G., Weber, M., and Zhang, G.: Validation of MIPAS-ENVISAT H<sub>2</sub>O operational data collected between July 2002 and March 2004, *Atmos. Chem. Phys.*, 13, 5791-5811, doi:10.5194/acp-13-5791-2013, 2013.

Yokouchi, Y., Noijiri, Y., Barrie, L. A., Toom-Sauntry, D., Machida, T., Inuzuka, Y., Akimoto, H., Li, H.-J., Fujinuma, Y., and Aoki, S.: A strong source of methyl chloride to the atmosphere from tropical coastal land, *Nature*, 403, 295–298, 2000.